People's Democratic Republic of Algeria

Ministry of Higher Education and Scientific Research

N°:……..

University Mohamed Boudiaf of M'Sila

Faculty of Technology

Department of Electronics

A Dissertation Submitted in Partial Fulfillment of

the Requirements for the Degree of Master in

Telecommunications Engineering

Assessing the Performance of Mean-Level CFAR Detectors in Gamma-Distributed Radar Clutter

Submitted by:
- Zakarya MENOUAR
- Mokrane BELFERROUM

Supervised by:

Dr. Mohamed SAHED

Defended on June 24, 2023 in front of the following board of examiners:

Elhadi KENANE	MCA	University of M'Sila	Chairman
Mohamed SAHED	MCA	University of M'Sila	Supervisor
Ali KHALFA	MCA	University of M'Sila	Examiner

Academic Year: 2022/2023


بسم الله الرحمن الرحيم

Dedications

I dedicate this milestone in my life

To my dearest mother.

You represent to me the source of tenderness and the example of

Devotion that has never ceased to encourage me.

To my dear father.

As an expression of my gratitude for the support, the

Sacrifices and all the efforts they made for my education.

To my dear brother

Abd El rahman

To my sister

Asma

To my niece

Zahia

To all my friends

"السواعد المتحدة"

"**Laith Tiger Fitness**"

To all the members of my extended family.

To my colleagues and teachers

To all those who have helped me in any way to accomplish this work.

Dedications

الحمد لله وكفى والصلاة على الحبيب المصطفى وأهله ومن وفى أما بعد:

الحمد لله الذي وفقنا لتثمين هذه الخطوة في مسيرتنا الدراسية بمذكرتنا هذه ثمرة الجهد والنجاح بفضله تعالى مهداة إلى:

من بسمتها غايتي و ماتحت أقدامها جنتي ..... إلى معنى الحب و الأمان و بسمة الحياة و سر الوجود....إلى أمي الغالية أطال الله في عمرها و بارك فيه.

إلى روح أبي الطاهرة أسكنه الله الفردوس الأعلى.

إلى من ترك بصمة في حياتي، أبي الثاني " جدي الغالي" رحمه الله وأسكنه الفردوس الأعلى.

إلى أمي الثانية المكافحة التي لا تستلم أبدا... التي أحبتني دون مقابل، علمتني القناعة و الرضا بما أملك....." جدتي الغالية"، أدامك الله لي وأطال في عمرك.

إلى من هو سندي وقوتي وضلعي الثابت الذي لا يميل إخوتي " يوسف، عائشة، زهرة ، نادية"،

و من هو قطعة من الأم و سند مثل الأب "خالي حسين، خالي مالك "حفظهم الله لي ورزقهم السعادة والهناء.

إلى خالتي حفظها الله و أبنائها " محمد سامي و هديل ".

إلى من تحلو الحياة برفقتهم أصدقائي.

بلفروم مقران

Acknowledgement

Above all, our thanks go to Allah the Almighty for giving us the health, strength and patience to accomplish this modest work... without Him nothing is done or created.

We would like to thank our parents for their moral support and encouragement.

Our warmest thanks go to our supervisor, **Dr. Mohamed SAHED**, for his guidance, support, advice and invaluable comments, which enabled us to overcome the difficulties and make progress in this study.

Our sincere thanks also go to **Dr. Elhadi KENANE**, for the honor he bestowed on us by agreeing to chair the examining board for this dissertation.

We would also like to express our sincere gratitude to **Dr. Ali KHALFA** for accepting the role of examiner on the jury and for the time he devoted to reading this manuscript.

Special thanks go to all the teachers in the Electronics Department at the University of M'Sila.

Z. MENOUAR

M. BELFERROUM

Abstract

In this study, we addressed the problem of adaptive detection of radar targets in a homogenous Gamma-distributed clutter. This type of detection is achieved by maintaining a Constant False Alarm Rate (CFAR) during the detection process. We assume that the radar uses a square-law device before the CFAR processor window. First of all, we present the fundamentals of radar detection of targets embedded in noise and giving the basics of CFAR detection. After that, we discuss in more details some Mean-Level CFAR detectors operating over a Gamma-distributed clutter, namely the CA- and GO-CFAR detectors. To do so, we carried out a complete theoretical analysis of both detectors. Indeed, closed-form expressions for the probability of false alarm (P_{fa}) have been presented for each detector. The calculation of the probability of detection (P_d), using the exact statistics of the cell under test (CUT), results in complicated integrals, which are hard to evaluate numerically. Thus, we propose approximate expressions for the probability of detection (P_d) for both detectors. These approximations are easier to compute and straightforwardly implementable in real-time applications. The obtained theoretical results are then tested and validated numerically by comparing them to their counterparts computed using numerical integrals and Monte-Carlo simulations, considering various scenarios. Moreover, a performance comparison of the studied detectors with the optimal detector has been made assuming a homogenous environment. The obtained results confirmed the efficacy of the CA-CFAR detector in the case of homogeneous environments.

Keywords: Radar, Adaptative CFAR detection, non-Gaussian Clutter, Gamma-Distribution, CA-CFAR, GO-CFAR.

Tables of Contents

List of Acronyms

RADAR	Radio Detection and Ranging
UE	Unbiased Estimator
IEEE	The Institute of Electrical and Electronics Engineers
ITU	The International Telecommunication Union
FAR	False Alarm Rate
CFAR	Constant False Alarm Rate
CUT	Cell Under Test
SNR	Signal-to-Noise Ratio
SCR	Signal-to-Clutter Ratio
ICR	Interference-to-Clutter Ratio
iid	Independent and identically distributed
r.v.	Random Variable
PDF	Probability density function
CDF	Cumulative distribution function
RF	Radio Frequency
EM	Electromagnetic
PPI	Plan Position Indicator
CW	Continuous-Wave,
RCS	Radar Cross Section
MLE	Maximum Likelihood Estimator
CA-CFAR	Cell Averaging CFAR
GO-CFAR	Greatest Of Selection Logic in Cell Averaging CFAR
SO-CFAR	Smallest Of Selection Logic in Cell Averaging CFAR

List of Symbols and Notations

$\Gamma(\alpha, \beta)$	Gamma distribution with parameters α and β.
$Exp(\mu)$	Exponential distribution with mean parameter μ.
$p_X = 2\sigma_X^2$	Mean Power of Clutter echo X
$p_Y = 2\sigma_Y^2$	Mean Power of target signal Y
μ	Arithmetic Mean
σ	Standard Deviation
σ^2	Variance
c	Shape parameter of the Weibull distribution
b	Scale parameter of the Weibull distribution or the K distribution
ν	Shape parameter of the K distribution
α	Shape parameter of the Gamma distribution
β	Scale parameter of the Gamma distribution
H_0	Null hypothesis of detection test that indicates target is absent
H_1	Alternative hypothesis of detection test that indicates target is present
Y	Target signal
X	Clutter (unwanted echo)
ϕ	Random Angle between X et Y
Z	Sufficient Statistic Test
Z_0	Signal in the CUT
N	Number of cells (observations) in one half of the reference window of a CFAR detector
$2N$	Number of cells (observations) in the reference window of a CFAR detector
P_d	Probability of Detection
P_{fa}	Probability of False Alarm
α_0	Desired Probability of False Alarm
X	Random variable
x	Particular observation of the random variable X
$f_X(x)$	Probability density function, PDF
$F_X(x)$	Cumulative Distribution Fonction, CDF
$f_{X\|Y}(x\|y)$	Conditional Probability density function of X given Y
$f_{Z_0}(z_0\|H_i)$	Conditional PDF of X under hypothesis H_i, $i = 1$ or 2.

$F_{Z_0}(z_0\|H_i)$	Conditional CDF of X under hypothesis H_i, $i = 1$ or 2.
T	Multiplication (or Scaling) Factor of a CFAR detector
λ_{CA}	Detection threshold of the CA-CFAR detector
λ_{GO}	Detection threshold of the GO-CFAR detector
λ_{SO}	Detection threshold of the SO-CFAR detector
$\Gamma(\cdot)$	Gamma Function of Euler
$K_v(\cdot)$	Modified Bessel Function of the second kind of order v
dB	Decibel
GHz	Giga Hertz

List of Figures

List of Tables

Introduction

A. Preamble

The technological advances in electronics and computer sciences have greatly contributed to the progress of radar communication systems. The main function of such system is to detect a target at a given range using transmitted and reflected high-frequency radio (or Electromagnetic, EM) waves. In fact, the word "radar" is an acronym for "***ra****dio* ***d****etection* ***a****nd* ***r****anging*". Thus, radar detection has become one of the main applications of radar signal processing that has attracted a great deal of attention over the years.

B. Historical Background

The history of radar began more than one hundred and fifty years ago, with the researches of the British physicist James Clerk Maxwell, in 1864. Maxwell showed theoretically that radio waves possess some properties resembling those of light waves. This was proved experimentally later in 1886 by the German physicist Heinrich Rudolf Hertz. As predicted theoretically by Maxwell, Hertz discovered and showed that the EM waves traveled at the speed of light and could be reflected, refracted, diffracted from various objects, and can be polarized like visible light waves.

The amazing discovery inspired researchers across the world. In 1901, the Italian inventor Guglielmo Marconi successfully sent radio signals across the Atlantic. This was the birth of modern communications industry. In 1904, the German engineer Christian Hulsmeyer first proposed the use of radio echo in a detection device to avoid collisions in navigation [1, 2]. Then, in 1917, Nikola Tesla developed the theoretical foundations for the future radar. Later, during the Second World War, Sir Robert Watson-Watt was able to build a radio detector that the Americans named "RADAR", which stands for "RAdio Detection And Ranging". During the following years, various

experimenters in EM waves has been carried out, which contributes to the gradual development of radar [1, 2].

For more in-depth information about radar history, the reader is invited to consult the book of Robert Buderi entitled *The Invention that Changed the World* [3].

C. Motivations

As mentioned before, radar target detection is a topic of great importance in various civil and military fields. Nowadays, the demand of more sophisticated detection algorithms has been increased significantly especially with the huge progress made in radar system electronics. It is well known that radar systems are operating in open environment and will receive returns echoes from many sources. In addition to reflections from targets (objects of interest), the radar signal includes unwanted echoes, known as *clutter,* backscattered from the environment and other unwanted objects. Thus, the radar system inevitably processes target signal in the presence of undesired clutter.

Indeed, clutter is a random process, which is the main source of detection errors. Thus, separating the target signal from the clutter is a key task, which will help significantly to mitigate the effect of these errors. To do so, a good mathematical and physical description of clutter is essential. Due to random nature of clutter, the theory of probability, which is a branch of mathematics, represents the natural framework for radar detection problem. It has been also shown that statistical modeling by means of probability distributions can provides a physical context for relating the characteristics of clutter to its random behavior. Thus, statistical clutter modeling is essential and basic for calculating and optimizing the performance of radar detectors.

D. State of the Art

A number of non-Gaussian models has been proposed in the literature to describe the random behavior of modern clutter, such as Log-normal, Weibull, Positive Alpha-Stable, Pareto, and *K* distributions [4] [5] [6] [7]. These models have been widely used to study the problem of constant false alarm rate (CFAR) detection [4] [5] [6] [7] [8] [9] [10]. It is well known that, whatever the adopted model, the performance of any CFAR detector can be effectively controlled by using two key metrics: the probability of detection (P_d) and the probability of false alarm (P_{fa}). However, closed-form expressions for these two metrics are not always available, due to the mathematical complexity that surrounds the use of non-Gaussian models. Therefore, it is important to look for non-Gaussian distributions that describe the clutter very well, and allow designing CFAR detectors whose P_{d} and P_{fa} are preferably expressed in closed-forms.

Recently, the Gamma distribution has been validated as a statistical model for high-resolution clutter collected by X-band maritime radar with low-grazing angles [11]. Performance analysis of some CFAR detectors assuming a Gamma distributed clutter has also been examined and discussed in [7] [11]. For instance, Zhou et al. introduced the CA-CFAR and the GO-CFAR schemes considering a homogenous background scenario [11]. One of their major contributions was the derivation of the expressions of the Pfa for both considered CFAR schemes. Unfortunately, these expressions were given in form of integrals, see e.g., Eqs. (19) and (22) in [11]. The authors of paper [11] claimed that these integrals cannot be expressed in simple closed-forms, but are readily evaluated numerically. Herein, motivated by the need to develop more practical CFAR detectors, we show in the present work that one can reduce both integrals to two exact closed-form expressions. These exact expressions for the P_{fa} of

CA- and GO-CFAR detectors are given in terms of the Gauss hypergeometric function and the second Appell function, respectively. To the best of our knowledge, it is worth noting also that we provide an original use of some approximations of the probability of detection for both detectors. This is the main contribution of this dissertation.

E. Organization of the Dissertation

This dissertation analyses the performance of some radar CFAR detection approaches operating over a Gamma-Distributed clutter, beginning with the theoretical concept and concluding with a simulated implementation.

In Chapter 1, a general description of the process begins by providing some fundamentals of radar detection in noise. Chapter 2 describes analytically some Mean-Level CFAR detectors and gives the mathematical derivations of the probability of false alarm and the probability of detection for each detector. In Chapter 3, we validate, test and examine the performance of such detectors via numerical simulations. The obtained results are discussed and interpreted in the same chapter, as well. At the end of the dissertation, we give some conclusions and recommends future works.

Chapiter 1 : Fundamentals of Signal Detection in Noise

1.1 Introduction

Signal detection in noise is a fundamental problem in signal processing, where the goal is to extract a weak signal from a noisy background [12]. It is a challenging task because noise can obscure the signal and make it difficult to distinguish. This problem is crucial in applications like radar, sonar, communications, and medical imaging, where the signal is often buried in noise caused by various sources. Various techniques, from simple threshold-based methods to advanced statistical and machine learning approaches, are used for signal detection. Advancements in this field have the potential to unlock new capabilities in areas like remote sensing.

1.2 Decision theory

The statistical decision theory is employed in various fields like radar, sonar, digital communication, and ultrasonic imaging with the objective of distinguishing between signals containing information and those that have noise or interference [12]. In a binary detection scenario, the observations are split into two sets that are mutually exclusive: the null hypothesis, H_0, containing noise samples (also called clutter), and the alternative hypothesis, H_1, containing both signal (target) and noise. When deciding between these two hypotheses, two types of errors can occur: a false alarm, which is when H_0 is accepted when it is true, and a miss, which is when H_0 is accepted when H_0 is true. The statistical models of the two hypotheses and the detector's design significantly influence these errors.

Classical detection theory assumes or has prior knowledge of the probability distribution functions of the two hypotheses [13]. The detector design can be determined using the Bayes likelihood ratio based on these functions. When given the a

priori density functions of the random variable X and an observed value $\varkappa$, the optimal detector's form is determined by the likelihood ratio, L($\varkappa$) [12] [14]:

$$L(x) = \frac{f_X(x|H_1)}{f_X(x|H_0)} \tag{1.1}$$

The statement is saying that there are two conditional probability densities, $f_X(\mathrm{x}|H_1)$ and $f_X(x|H_0)$), which describe the probability of an event X given two different conditions, H_1 and H_0. A decision is then made by comparing a test statistic called $L(x)$to a threshold value called λ. This threshold value is chosen based on how well the detector is expected to perform.

$$L(x) = \begin{cases} > \lambda & accept\ H_1 \\ \leq \lambda & accept\ H_0 \end{cases} \tag{1.2}$$

The statement explains that if an equality condition is met, a random decision-making rule can be used. This rule is usually equally likely to choose between two hypotheses, but may be biased based on the detector's performance criteria or the associated cost of each hypothesis. Currently, the equality condition is set for H_0 to reduce the chances of incorrectly accepting H_1, which is crucial as further discussed later on.

The detector's effectiveness in detecting errors depends on the threshold set to either fix the probability of a false alarm or the probability of a miss. Typically, having a false alarm is more worrisome than a miss because accepting hypothesis H_1 could have serious consequences. Therefore, selecting an optimal threshold λ for the detector requires considering the restrictions on the probability of false alarms. The probability of false alarm,P_{fa} , can be found by the Neyman-Pearson criteria [14]:

$$P_{fa} = \int_{\lambda}^{\infty} P\big(L(x|H_0)\big)\, dL(x) \leq \alpha \quad for\ all\ x \tag{1.3}$$

The size of the detector, which is referred to as quantity α, is a fixed parameter. This means that regardless of the observations x, the probability of false alarm will never go beyond a certain level. This is called constant false alarm rate (CFAR) analysis, which is used as an optimizing constraint in various detectors discussed in this thesis. It is important to note that the threshold for detecting the target is not based on any information about the target itself. Therefore, the detector's probability of detecting the target may vary depending on the distribution of the target.

Although the likelihood of committing a type I error, which is below a specified level α, is certain for all observations that fall under the null hypothesis, H_0, the occurrence of a type II error depends on the statistics of the alternative hypothesis, H_1. To calculate the probability of a missed detection, also known as a type II error, denoted as P_m, one needs to evaluate the integral of the test statistic presented in (1.2), that is [12],

$$P_m = \int_{-\infty}^{\lambda} P\big(L(x|H_1)\big)\, dL(x) = 1 - \beta \tag{1.4}$$

The probability of missing a target is represented by $1 - \beta$, while the probability of detecting it, denoted as P_d, is simply represented by β. The probability of detection depends on the threshold λ, which is predetermined by the statistics associated with the null hypothesis and is chosen to meet the CFAR constraint. This means that the performance of a detector, in terms of probability of detection, cannot be improved for a fixed size α independent of the target statistics [15] [16] [10].

1.3 Statistical clutter models

This section will introduce the different statistical models of sea clutter found in literature, and extensively discuss the properties that explain the random nature of radar clutter. However, to avoid making this manuscript too lengthy, the experimental validation of these statistical models will not be covered in this dissertation. For further information on the experimental modeling and validation of sea clutter, please refer to the literature. Table 2.1 presents a summary of the main distinctions between noise and clutter returns, which are modeled differently due to their unique characteristics. It has been noted that these two phenomena have distinct properties [17].

Table 1.1 - Clutter versus Noise

Noise Signal	**Clutter Signal**
Amplitude is independent of the transmitted radar signal	Amplitude is proportional to the transmitted signal
Wide bandwidth	Narrow bandwidth
Independent of environmental parameters	Can vary with changing environmental conditions

1.3.1 Gaussian clutter models

1.3.1.1 Normal Distribution

The probability density function (pdf) describes the characteristics the normal distribution, also known as the Gaussian distribution, is defined as follows:

$$f_X(x) = \frac{1}{\sqrt{2\pi\sigma}} \exp\left(-\frac{(x-\mu)^2}{2\sigma^2}\right) \tag{1.5}$$

where μ is the mean and $2\sigma^2$ is the variance of X. The pdf of the normal distribution is represented in Figure 1.3.

Using the definition of the error function, the cumulative distribution function (cdf) can be given as follows

$$F_X(x) = \frac{1}{2} + \frac{1}{2} erf\left(\frac{x-\mu}{\sigma\sqrt{2}}\right) \tag{1.6}$$

The moments about the mean of this distribution are

$$E[X^n] = \begin{cases} 0 & for\ n\ odd \\ \dfrac{n!\,\sigma^n}{\left(\frac{n}{2}\right)!\,2^{\frac{n}{2}}} & for\ n\ even \end{cases} \tag{1.7}$$

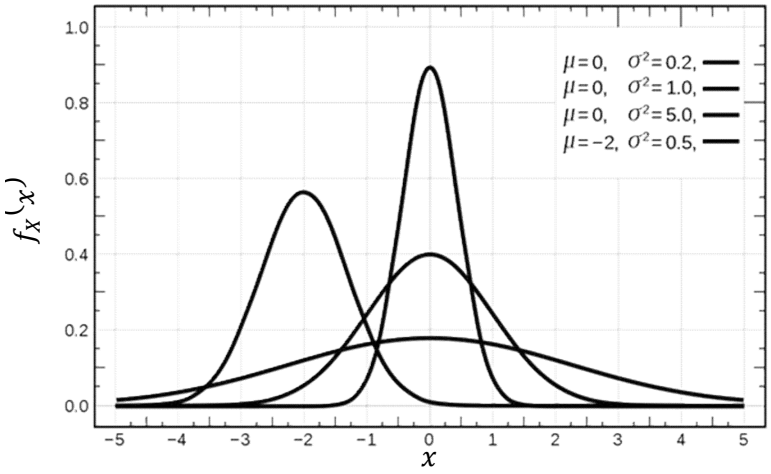

Figure 1.1 - Probability density function of the Gaussian distribution

1.3.1.2 Rayleigh Distribution

The Rayleigh distribution is one of the Gaussian models, and it is defined by the following pdf, which is depicted in Figure 1.2.

$$f_X(x) = \frac{x}{b^2}\exp\left(-\frac{x^2}{2b^2}\right), \qquad x > 0 \tag{1.8}$$

and the corresponding cumulative distribution function is given by

$$F_X(x) = 1 - \exp\left(-\frac{x^2}{2b^2}\right), \qquad x > 0 \tag{1.9}$$

where b is the scale parameter of the Rayleigh distribution.

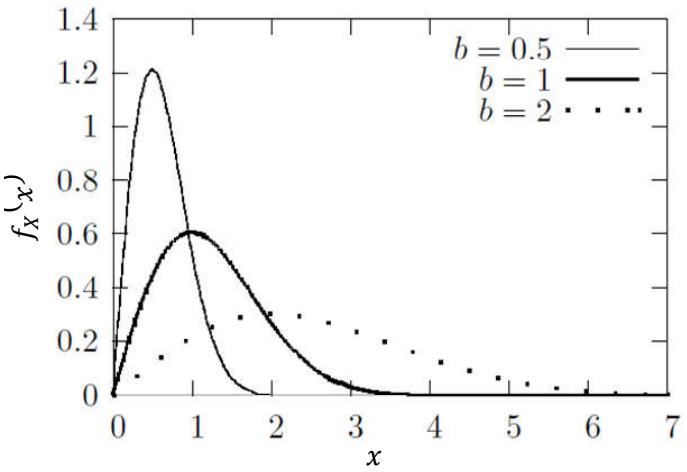

Figure 1.2 - Probability density function of the Rayleigh distribution

1.3.2 Non-Gaussian clutter models

1.3.2.1 Lognormal Distribution

The lognormal distribution of a random variable X is given by

$$f_x(x) = \begin{cases} \frac{1}{\sqrt{2\pi}x\sigma} exp\left(-\frac{(\ln(x)-\mu)^2}{2\sigma^2}\right), x \geq 0 \\ 0\ ; \qquad\qquad otherwise \end{cases} \tag{1.10}$$

where μ is the mean and $2\sigma^2$ is the variance of the lognormal distribution. The corresponding cdf can be expressed simply in terms of the error function, as follows

$$F(x) = \frac{1}{2}\left(1 + \text{erf}\left(\frac{\ln(x) - \mu}{\sigma\sqrt{2}}\right)\right. \tag{1.11}$$

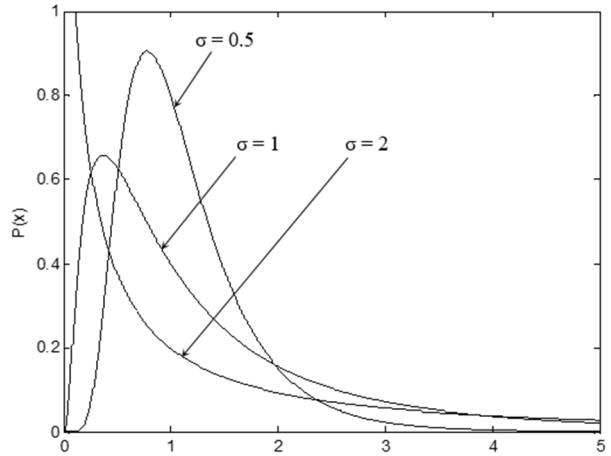

Figure 1.3 - Probability density function of the lognormal distribution

1.3.2.2 Weibull-Distribution model

A random variable X is said to have a Weibull-distribution, as shown in Figure 1.2, if its probability density function is given by

$$f_X(x) = \begin{cases} \frac{c}{b}\left(\frac{x}{b}\right)^{c-1} exp\left(-\left(\frac{x}{b}\right)^{c}\right), & x > 0,\ a > 0,\ and\ b > 0 \\ 0 & otherwise \end{cases} \tag{1.12}$$

where c and b are the shape and the scale parameters of the Weibull-distribution respectively.

The corresponding cdf is given by

$$F(x) = 1 - exp\left(-\left(\frac{x}{b}\right)^{c}\right) \tag{1.13}$$

The n-th moments of the Weibull distribution can be given by

$$m_n = b^n \Gamma\left(\frac{n}{c} + 1\right) \tag{1.14}$$

and consequently, the mean and variance of this distribution are, respectively,

$$E(x) = b\,\Gamma\left(\frac{1}{c} + 1\right) \tag{1.15}$$

$$Var(x) = b^2\left[\Gamma\left(\frac{2}{c} + 1\right) - \Gamma^2\left(\frac{1}{c} + 1\right)\right] \tag{1.16}$$

where $\Gamma(\cdot)$ denotes the Gamma function.

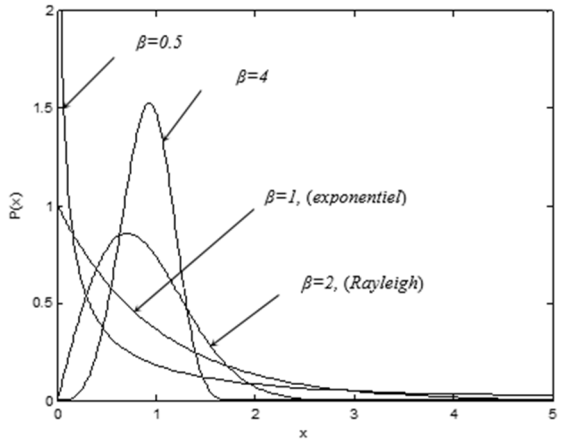

Figure 1.4 - Probability density function of the Weibull-distribution

1.3.2.3 *K*-Distribution

The primary purpose of the *K*-distribution is to depict radar sea clutter. It is used to model a random variable X, which has a probability density function

$$f_x(x) = \begin{cases} \frac{4}{b\Gamma(v)}\left(\frac{x}{b}\right)^v K_{v-1}\left(\frac{2}{b}x\right), x \geq 0 \\ 0 \qquad\qquad\qquad\qquad , otherwise \end{cases} \tag{1.17}$$

where α and β are the shape and the scale parameters of the Gamma-distribution respectively, and $\Gamma(\alpha)$ denotes the Gamma function.

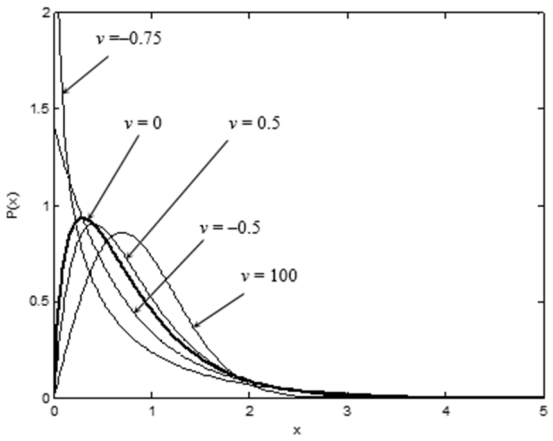

Figure 1.5 - Probability density function of the *K*-Distribution

1.3.2.4 Gamma-Distribution

The Gamma distribution is validated as a statistical model for high-resolution radar clutter. Its pdf is defined by

$$f(x: \alpha, \beta) = \frac{\beta^\alpha}{\Gamma(\alpha)} x^{\alpha-1} e^{-\beta x} \tag{1.18}$$

where α and β are the shape and the scale parameters of the Gamma-distribution respectively, and $\Gamma(\alpha)$ denotes the Gamma function.

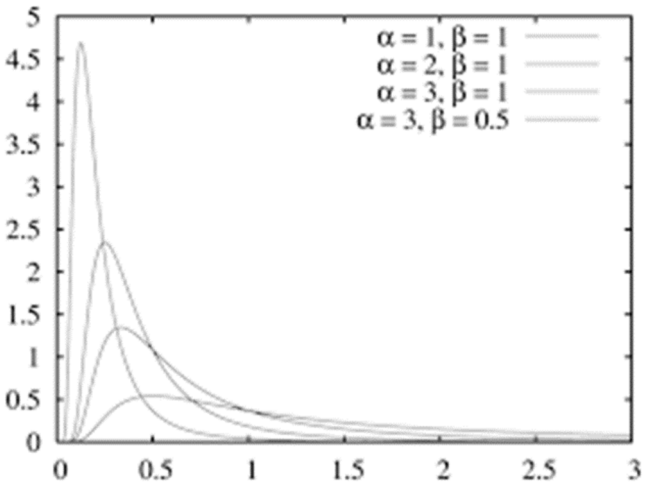

Figure 1.6 - Probability density function of the Gamma-distribution

1.4 Target signal models

In this section, we will discuss the models of different types of radar targets. Indeed, this is based on the concept of radar cross sections (RCS) for simple point targets and extends to more complicated cases of targets with multiple scattering centers. In general, targets scatter energy in all directions; the RCS, denoted by y, is a function of the incident angle, the scattering angle, and the signal frequency. RCS also depends on the shape of the target and the materials it's made of [18] [19].

Because the radar system and the target may be moving, the RCS value can change over time. This causes targets to fluctuate. To simulate fluctuating targets, four statistical models, referred to as Swerling 1 through Swerling 4, are widely adopted in practice. The Swerling models divide fluctuating targets into two probability distributions and two time-varying behaviors (see Table 1.2).

Table 1.2 - Swerling Target Models

Case	Probability Density Function	Fluctuation Period	Fluctuation Speed
Swerling I	Rayleigh	Dwell-to-Dwell	Slow fluctuating
Swerling II	Rayleigh	Pulse-to-Pulse	Fast fluctuating
Swerling III	Chi-square, degree 4	Dwell-to-Dwel	Slow fluctuating
Swerling IV	Chi-square, degree 4	Pulse-to-Pulse	Fast fluctuating

1.4.1 Swerling I model

In this case, Swerling I model describes a target whose magnitude of the backscattered signal is relatively constant during the dwell time. The RCS varies according to the Rayleigh-distribution given by

$$f_Y(y) = \frac{y}{\sigma_0^2} exp\left(-\frac{y^2}{2\sigma_0^2}\right) \tag{1.19}$$

where $2\sigma_0^2$ is the arithmetic mean of all values of RCS of the reflecting object.

1.4.2 Swerling II model

The Swerling II target models are similar to Swerling I models, using the same pdf, except in this case the RCS values changes faster and varies from pulse to pulse.

Both Swerling cases I and II can be applied to targets that are made up of many independent scatterers of roughly equal areas like airplanes. However, in Swerling case II there is no rotating surveillance antenna but a focused onto a target tracking radar.

1.4.1 Swerling III model

The Swerling III target is similar to Swerling I, but with four degrees of freedom. The RCS fluctuation follows the following distribution

$$f_Y(y) = \frac{9y^3}{2\sigma_0^4} exp\left(\frac{3y^2}{2\sigma_0^2}\right) \tag{1.20}$$

1.4.1 Swerling IV model

The Swerling IV model is similar to Swerling III, but the RCS varies from pulse to pulse rather than from scan to scan and follows (1.20).

1.5 Radar detection principles

Previously, we have observed that in order to apply Bayes' criterion, we need to have information about the a priori probabilities and cost assignments for all potential

decisions. However, if we are unable to determine the a priori probabilities, the minimax criterion can be utilized. It is often challenging to assign realistic costs and a priori probabilities in certain physical scenarios, such as radar detection. To address this issue, we utilize the conditional probabilities of false alarm P_{fa} and detection P_d. The Neyman-Pearson test mandates that we fix P_{fa} to a specific value α_0 while maximizing P_d. Since $P_m = 1 - P_d$, maximizing P_d is the same as minimizing P_m.

To ensure that $P_{fa} = \alpha_0$ and minimize P_m (maximize P_d), we utilize the calculus of extrema and construct an objective function called J [20]:

$$J = P_m + \lambda\left(P_{fa} + \alpha_0\right) \tag{1.21}$$

where $\lambda \geq 0$ is the Lagrange multiplier.

It is important to note that there are various decision regions, Z_1, within the observation space Z that satisfy the constraint $P_{fa} = \alpha_0$. The goal is to identify the decision regions that result in the minimum P_m. Therefore, we modify the objective function J to be expressed in terms of the decision region.

$$J = \int_{Z_1} f_Y(y|H_1)dy + \lambda\left[\int_{Z_0} f_Y(y|H_0)dy - \alpha_0\right] \tag{1.22}$$

As a result, the decision region Z_1 should be assigned values that satisfy $f_Y(y|H_1) > f_Y(y|H_0)$ to minimize the objective function J. Consequently, the decision rule can be defined as follows [14]

$$\Lambda(y) = \frac{f_Y(y|H_1)}{f_Y(y|H_0)} \underset{H_0}{\overset{H_1}{\gtrless}} \eta \tag{1.23}$$

The threshold value η obtained from the Bayes' criterion is the same as the Lagrange multiplier λ in the Neyman-Pearson $(N-P)$ test where the false alarm probability is set to a specific value α_0. If we define the conditional density of Λ given that $H_0$is true as $f_\Lambda(\lambda|H_0)$, then we can express $P_{fa} = \alpha_0$ as [14]

$$P_{fa} = \int_{Z_1} f_Y(Y|H_0)\, dy = \int_{\lambda}^{\infty} f_\Lambda[\lambda(y)|H_0]\, d\lambda \tag{1.24}$$

If the probability of rejecting H_0 in a test is exactly α_0, then it is referred to as the most powerful test of level α_0.

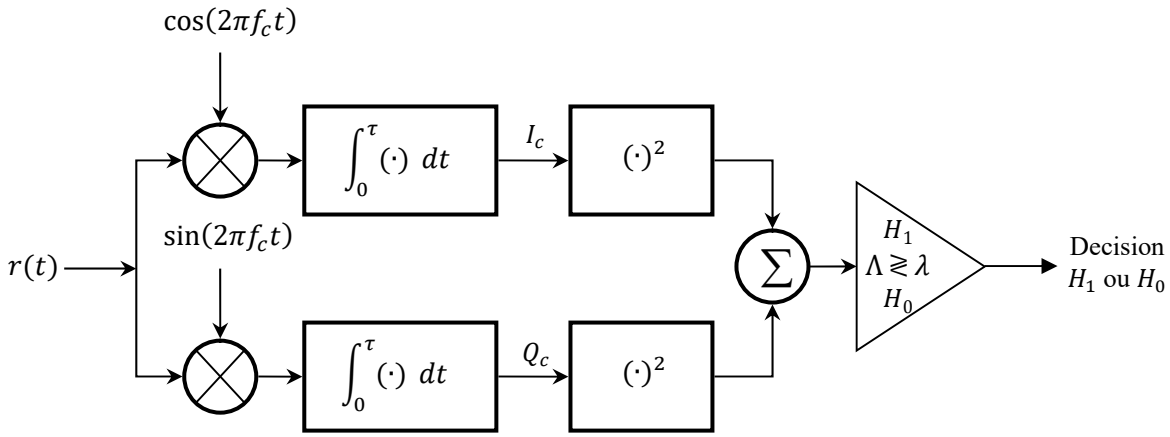

Figure 1.7 - Optimal Neyman-Pearson quadratic detector

1.6 CFAR Detection

In the case of homogeneous clutter, the M samples $x_1, x_2, \ldots\ldots, x_M$ in the M neighboring cells of the reference window of the CFAR detector are statistically independent and identically distributed (iid), and are independent of the CUT statistic z_0. A statistical test, denoted Z, is formed from the samples $x_1, x_2, \ldots\ldots, x_M$, which represents an estimate of the average power level of the clutter in the CUT. This estimate is multiplied by a thresholding constant T, which is chosen so as to guarantee a

certain desired false alarm probability $P_{fa}(T) = \alpha_0$. This results in an adaptive detection threshold. To make a decision on the presence or absence of a target in the CUT, the content of the latter, denoted Z_0, is compared to the threshold adaptive according to the following binary decision rule [15, 16, 18]

$$Z_0 \underset{H_0}{\overset{H_1}{\gtrless}} TZ \tag{1.25}$$

The CFAR detector uses a binary decision rule to compare the content of the CUT, denoted Z_0, with an adaptive detection threshold, which is totally independent of the clutter parameters to ensure a constant false alarm rate. The detection threshold is calculated based on the pdfs of the two statistic $Z_0 \,|\, H_0$ and Z. To evaluate the performance of a CFAR detector, the false alarm probability, P_{fa}, and the detection probability, P_d, are often used. The pdfs of the statistical test Z, and the content of the CUT, Z_0, under the two hypotheses H_0 and H_1 respectively, are used to calculate P_{fa} and P_d, as follows [14]

$$P_{fa} = \Pr(Z_0 > TZ|H_0) = \int_0^\infty \left[\int_{Tz}^\infty f_{Z_0|H_0}(z_0|H_0) dz_0 \right] f_Z(z) dz \tag{1.26}$$

and

$$P_d = \Pr(Z_0 > TZ|H_1) \int_0^\infty \left[\int_{Tz}^\infty f_{Z_0|H_1}(z_0|H_1) dz_0 \right] f_Z(z) dz \tag{1.27}$$

It is difficult to determine the pdfs of the statistics Z, $Z_0|H_0$ and $Z_0|H_1$, which makes it challenging to calculate the false alarm probability and detection probability. In practice, the user specifies the desired false alarm probability, P_{fa}, denoted as α_0, and the detection threshold value is deduced accordingly.

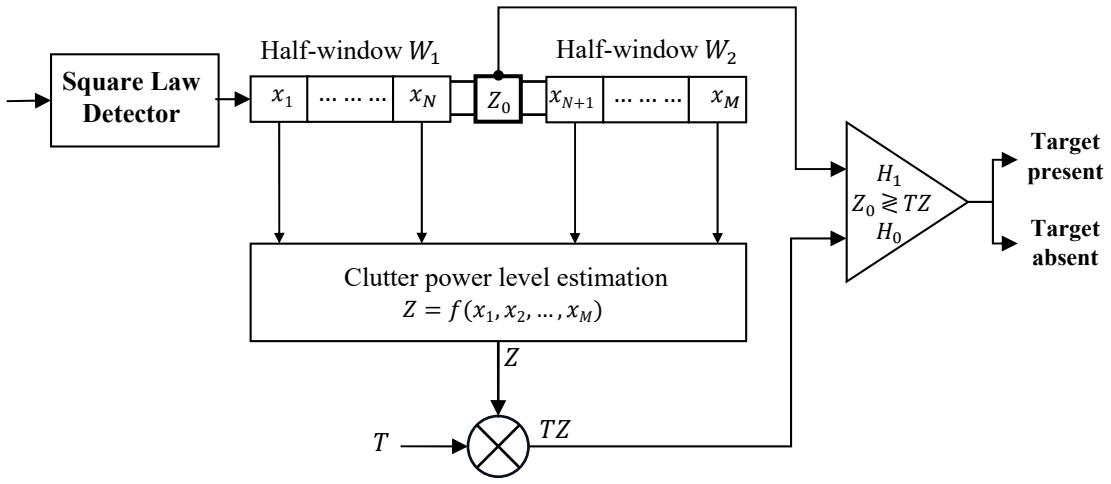

Figure 1.8 - Typical CFAR detection processor

1.7 Conclusion

In conclusion, the detection of signals in noise is a challenging problem that arises in many signal processing applications. The ability to reliably detect weak signals in the presence of noise is critical for many fields, including radar. Developing effective algorithms for signal detection in noise requires balancing sensitivity and specificity, and may involve exploiting various statistical and spectral properties of the signal and noise. Advances in this area have the potential to enable new capabilities and improve performance in a range of applications.

Chapiter 2 : CFAR Detection in Homogenous Gamma-Distributed Clutter

2.1 Introduction

In this chapter, we will examine and analyze the CFAR detection in homogenous Gamma-distributed (GM) clutter. In doing that, we introduce and study three well known CFAR processors, namely the Cell-Averaging (CA) CFAR, the Greatest-Of (GO) CFAR. As a part of our analysis, we will provide, for each detector, the fundamental aspect of its functioning and the corresponding probabilities of false alarm and detection (P_{fa} and P_{d}).

2.2 Statistics of the CUT

In this paragraph, we introduce the distribution that characterize the signal in the CUT under both hypothesis H_0 and H_1. For our analysis, we suppose that the radar system is equipped by a square-law detector before the CFAR window.

In practical situations, the CUT's content consists Z_0 either of clutter echo X only or a combination of clutter echo X and target signal return Y. In that case, the detection problem can be formulated as a binary hypothesis testing problem, which may be stated as follows [13] [19]

$$H_0(Clutter\ only): Z_0 = X \tag{2.1}$$

$$H_1(Target + Clutter): Z_0 = Y + X \tag{2.2}$$

where H_0 stands for the null hypothesis, which states that there is no target in the CUT (i.e., only clutter in the CUT), and H_1 is the alternative hypothesis, which states that there is a target and clutter in the CUT.

2.2.1 Statistics of the CUT under H_0

We assume that the content of the CUT Z_0 under H_0 is distributed according to the GM-distribution (here there is no target present in the CUT). Thus, the pdf and cdf of Z_0 in this case are given, respectively, by [11] [21]

$$f_{Z_0}(z_0|H_0) = \frac{\beta^{\alpha}}{\Gamma(\alpha)} {z_0}^{\alpha-1} \exp(-\beta z_0) \tag{2.3}$$

And

$$F_{Z_0}(z_0|H_0) = \frac{\gamma(\alpha, \beta z_0)}{\Gamma(\alpha)} \tag{2.4}$$

2.2.2 Statistics of the CUT under H_1

Under hypothesis H_1, the content of the CUT Z_0, defined by (3.2), is due to both target returns Y and clutter echoes X. Specifically, we assume throughout this dissertation a Swerling I or II fluctuating target whose pdf and cdf are given, respectively, by

$$f_Y(y;\sigma_Y) = \frac{1}{2\sigma_Y^2} \exp\left(-\frac{y}{2\sigma_Y^2}\right) \tag{2.5}$$

and

$$f_Y(y;\sigma_Y) = \frac{1}{2\sigma_Y^2} \exp\left(-\frac{y}{2\sigma_Y^2}\right) \tag{2.6}$$

where σ_Y^2 is the variance of the in-phase and in-quadrature Gaussian components of the target signal Y, and $2\sigma_Y^2$ the average of the target signal power.

By knowing the appropriate models of target signal returns given by (2.6) and clutter echoes, we can now look for the distribution of Z_0 under H_1. Since the signal in

the CUT is a combination of target and GM distributed clutter, it is difficult to calculate analytically the pdf of the CUT's content under H_1. For a square-law detector, the complex envelope of the target signal $\boldsymbol{S}$ is added to the complex envelope of clutter echo $\boldsymbol{C}$, and the resulted complex signal is then squared. Accordingly, the CUT output Z_0 can be modelled as the square of the resulted complex signal modulus, which can be given as [22]

$$\begin{aligned} Z_0 \triangleq |\boldsymbol{S}+\boldsymbol{C}|^2 &= |\boldsymbol{S}|^2 + |\boldsymbol{C}|^2 + 2|\boldsymbol{S}||\boldsymbol{C}|\cos(\varphi) \\ &= Y + X + 2\sqrt{Y}\sqrt{X}\cos(\varphi) \end{aligned} \tag{2.7}$$

where $|\cdot|$ is the complex modulus, $Y = |\boldsymbol{S}|^2$, $X = |\boldsymbol{C}|^2$ and φ is a random variable (rv) uniformly distributed on the interval $[0,\ 2\pi]$, which represents here the phase between $\boldsymbol{S}$ and $\boldsymbol{C}$.

Unfortunately, a closed-form expression for the pdf of Z_0 under hypothesis H_1 cannot be derived, which complicates significantly the analysis. Thus, for convenience, we assume that the pdf of clutter in the CUT will be approximated by an exponential distribution with exact same mean power as that of the GM-distributed clutter. Accordingly, the content of the CUT, under H_1, is reduced to the sum of an exponential fluctuating target and an exponential distributed clutter. This approximation has demonstrated high accuracy, which makes it commonly used in the literature [23]. In such case, the resulting signal in the CUT will be also exponentially distributed, and its corresponding conditional pdf can be expressed as

$$f_{Z_0}(z_0|H_1) = \frac{1}{2\sigma_X^2 + 2\sigma_Y^2}\exp\left(-\frac{z_0}{2\sigma_X^2 + 2\sigma_Y^2}\right) \tag{2.8}$$

where $2\sigma_X^2 = \alpha/\beta$ is the mean power of GM-distributed clutter in the reference cells, and $2\sigma_Y^2$ is the mean power of the exponentially fluctuating target. Now, the signal-to-clutter ratio (SCR) can be defined as

$$\text{SCR} \triangleq \frac{2\sigma_Y^2}{2\sigma_X^2} = \frac{2\sigma_Y^2}{\alpha/\beta} \tag{2.9}$$

Hence, the pdf and cdf of $Z_0|H_1$ can be given in terms of SCR, respectively, by

$$f_{Z_0}(z_0|H_1) = \frac{\beta}{\alpha(1+\text{SCR})}\exp\left(-\frac{\beta z_0}{\alpha(1+\text{SCR})}\right) \tag{2.10}$$

And

$$F_{Z_0}(z_0|H_1) = 1 - \exp\left(-\frac{\beta z_0}{\alpha(1+\text{SCR})}\right) \tag{2.11}$$

2.3 Optimal fixed threshold detector

In the Neyman-Pearson framework, an optimal detector for detecting a target in a homogenous background with parameters, which are known *a priori* (i.e., known power) uses a fixed detection threshold, λ. To determine the presence of the target, the signal value Z_0 in the CUT is compared simply to λ, according to the following decision rule

$$Z_0 \underset{H_0}{\overset{H_1}{\gtrless}} \lambda \tag{2.12}$$

2.3.1 P_{fa} of the optimal fixed threshold detector

In the absence of a target in the CUT (i.e, under H_0), Z_0 follows a GM-distribution with parameters α and β. Therefore, the probability of false alarm of the optimal detector (P_{fa}^{Op}) can be determined by

$$\begin{aligned} P_{fa}^{Op} &= \Pr(Z_0 > \lambda | H_0) = \int_{\lambda}^{\infty} f_{Z_0}(z_0|H_0)dz_0 \\ &= 1 - F_{Z_0}(\lambda|H_0) = 1 - \frac{\gamma(\alpha, \beta\lambda)}{\Gamma(\alpha)} \end{aligned} \tag{2.13}$$

In order to obtain the value of the fixed threshold λ of the optimal detector, for a desired $P_{fa} = \alpha_0$, equation (3.12) must be inverted numerically.

2.3.2 P_d of the optimal fixed threshold detector

In the presence of a target in the CUT, $Z_0|H_0$ follows the exponential distribution defined by (2.10). Therefore, the probability of detection of the optimal detector (P_d^{Op}) can be determined by

$$\begin{aligned} P_d^{Op} &= \Pr(Z_0 > \lambda | H_1) = \int_{\lambda}^{\infty} f_{Z_0}(z_0|H_1)dz_0 \\ &= 1 - F_{Z_0}(\lambda|H_1) = \exp\left(-\frac{\beta\lambda}{\alpha(1+\mathrm{SCR})}\right) \end{aligned} \tag{2.14}$$

2.4 Cell Averaging CFAR detector

In this paragraph, we will analyze the performance of the Cell Averaging (CA) CFAR detector in presence of GM-distributed clutter. The bloc diagram of the CA-CFAR detector is shown in Figure 3.1 [11].

Let us consider a set $\{x_i : i = 1, 2, \ldots, 2N\}$ of $2N$ independent and identically distributed (*iid*) GM random variables, which represent in our case a $2N$ radar clutter

observations located in the reference window of a given CFAR detector. In the case of CA-CFAR processor, the decision rule is defined as follows [11]

$$Z_0 \underset{H_0}{\overset{H_1}{\gtrless}} TZ_{CA} \tag{2.15}$$

where $Z_{CA} = \sum_{i=1}^{2N} X_i$ is a sufficient statistic of clutter power level, whose pdf can be expressed, according to [11], by

$$f_{Z_{CA}}(z) = \frac{\beta^{2N\alpha}}{\Gamma(2N\alpha)} z^{2N\alpha-1}\ e^{-\beta z} \tag{2.16}$$

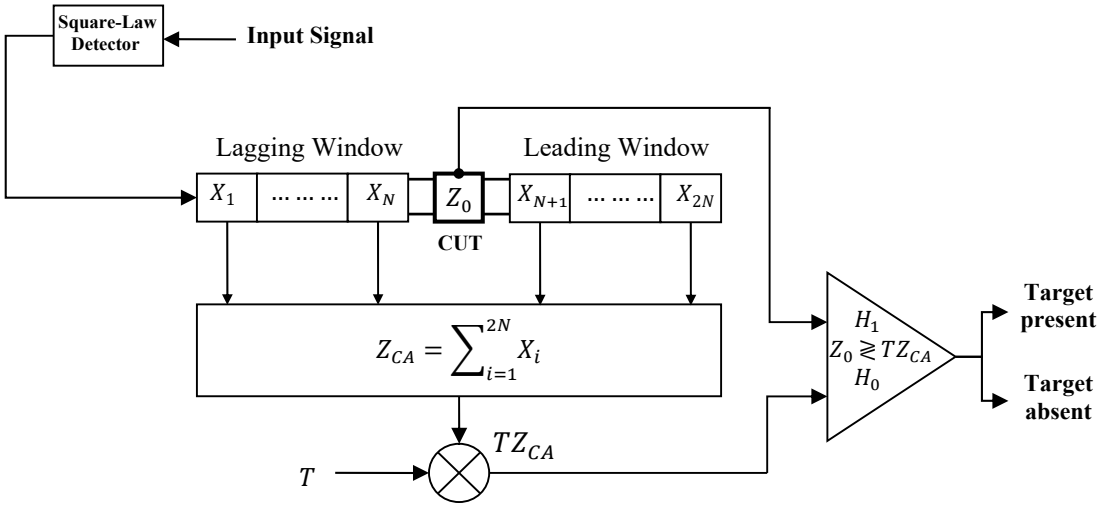

Figure 2.1 - Block diagram of the CA-CFAR detector

2.4.1 P_{fa} of the CA-CFAR detector

The false alarm probability (P_{fa}) of the CA-CFAR detector can be obtained by replacing (2.3) or (2.4) and (2.15) into (1.26), and it can be given as [7]

$$P_{fa}^{CA} = \frac{\Gamma\big(\alpha(2N+1)\big)T^{\alpha}}{\Gamma(2N\alpha+1))\Gamma(\alpha)(1+T)^{\alpha(2N+1)}}\ {}_2F_1\left(1, \alpha(2N+1); 2N\alpha+1; \frac{1}{1+T}\right) \tag{2.17}$$

where ${}_2F_1(\cdot,\cdot;\cdot;\cdot)$ denotes the Gauss hypergeometric function [24].

2.4.2 P_d of the CA-CFAR detector

The detection probability (P_d) of the CA-CFAR detector can be obtained by replacing (2.10) or (2.11) and (2.15) into (1.27) as follows

$$\begin{aligned}
P_d^{CA} &= \Pr(Z_0 > TZ_{CA}|H_1) \\
&= \int_0^\infty \left[\int_{Tz}^\infty f_{Z_0}(z_0|H_1)dz_0 \right] f_{Z_{CA}}(z)dz \\
&= 1 - \int_0^\infty F_{Z_0}(Tz|H_1) f_{Z_{CA}}(z)dz \\
&= 1 - \int_0^\infty \left(1 - \exp\left(-\frac{\beta Tz}{\alpha(1+\mathrm{SCR})}\right)\right) f_{Z_{CA}}(z)dz \\
&= \int_0^\infty \exp\left(-\frac{\beta Tz}{\alpha(1+\mathrm{SCR})}\right) f_{Z_{CA}}(z)dz \\
&= \frac{\beta^{2N\alpha}}{\Gamma(2N\alpha)} \int_0^\infty z^{2N\alpha-1} \exp\left(-\frac{\beta Tz}{\alpha(1+\mathrm{SCR})} - \beta z\right) dz \\
&= \frac{1}{\Gamma(2N\alpha)} \int_0^\infty z^{2N\alpha-1} \exp\left(-\left(1 + \frac{T}{\alpha(1+\mathrm{SCR})}\right) z\right) dz
\end{aligned} \tag{2.18}$$

This last integral can be solved using equation 3.381.4 of [25], which yields the following closed-form approximation for the P_d of the CA-CAFR detector

$$P_d^{CA} = \left(1 + \frac{T}{\alpha(1+\mathrm{SCR})}\right)^{-2N\alpha} \tag{2.19}$$

2.5 Greatest Of CFAR detector

Herein, we will analyze the performance of the Greatest Of (GO) CFAR detector in presence of GM-distributed clutter. The bloc diagram of the GO-CFAR detector is shown in Figure 2.2. The decision rule of this detector is defined as follows [11, 26]

$$Z_0 \underset{H_0}{\overset{H_1}{\gtrless}} TZ_{GO} \tag{2.20}$$

where $Z_{GO} = Max(U,V)$, and $U = \sum_{i=1}^{N} X_i$ and $V = \sum_{i=N+1}^{2N} X_i$ are two sufficient statistics of clutter power level, whose pdfs and cdfs can be expressed, respectively, by

$$f_U(z) \triangleq f_V(z) = \frac{\beta^{N\alpha}}{\Gamma(N\alpha)} z^{N\alpha-1} \exp(-\beta z) \tag{2.21}$$

$$F_U(z) \triangleq F_V(z) = \frac{\gamma(N\alpha, \beta z)}{\Gamma(N\alpha)} \tag{2.22}$$

According to [14], the pdf of Z_{GO} can be calculated as follows

$$f_{Z_{GO}}(z) = 2 f_U(z)\, F_U(z) \triangleq 2 f_V(z)\, F_V(z) \tag{2.23}$$

which yields

$$f_{Z_{GO}}(z) = \frac{2\beta^{N\alpha}}{\Gamma^2(N\alpha)} z^{N\alpha-1}\, \gamma(N\alpha, \beta z) \exp(-\beta z) \tag{2.24}$$

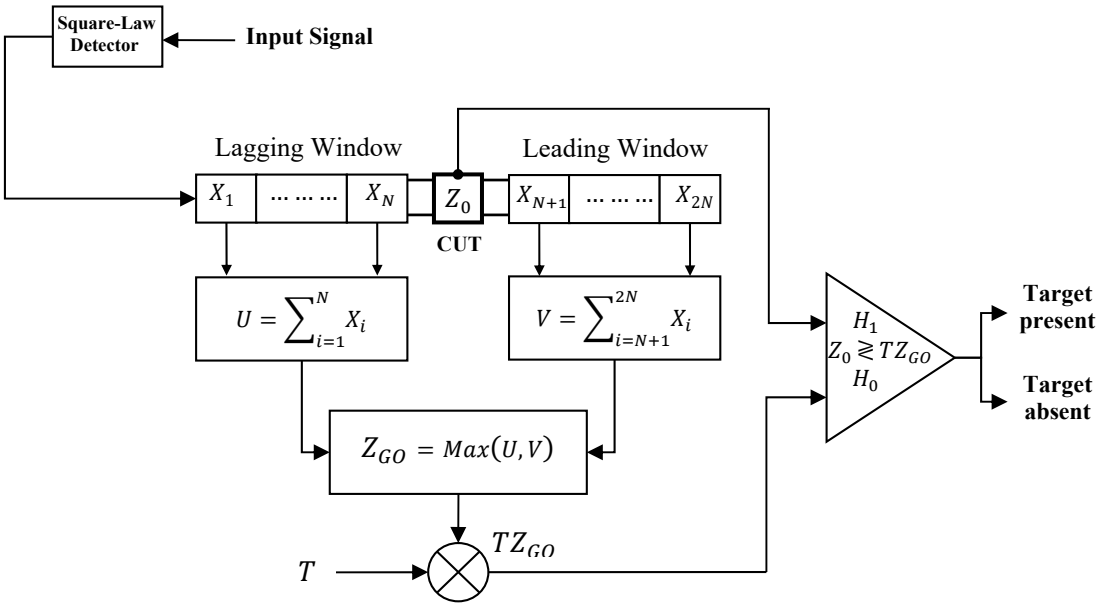

Figure 2.2 - Block diagram of the GO-CFAR detector

2.5.1 P_{fa} of the GO-CFAR detector

The false alarm probability (P_{fa}) of the GO-CFAR detector can be obtained by replacing (2.3) or (2.4) and (2.23) into (1.26), and it can be given as [7]

$$P_{fa}^{GO} = \frac{2}{\Gamma^2(N\alpha)}\left[\frac{\Gamma\left(\frac{1}{2}\right)\Gamma(2N\alpha)\Gamma(N\alpha)}{2^{2N\alpha}\Gamma(N\alpha 1\frac{1}{2})} - \frac{\Gamma(\alpha(2N+1))T_{GO}^{\alpha}}{N\alpha^2\Gamma(\alpha)(2+T_{GO})^{\alpha(2N+1)}}\right] \times F_2\left(\alpha(2N+1), 1,1; N\alpha+1, \alpha+1; \frac{1}{2+T_{GO}}, \frac{T_{GO}}{2+T_{GO}}\right) \tag{2.25}$$

where $F_2(a, b, \cdot;\cdot,\cdot;\cdot,)$ denotes the Gauss hypergeometric function [24, 27].

2.5.2 P_d of the GO-CFAR detector

Now, the detection probability (P_{d}) of the GO-CFAR detector can be obtained by replacing (2.10) or (2.11) and (2.23) into (1.27)

$$P_d^{GO} = \Pr(Z_0 > TZ_{GO}|H_1) \tag{2.26}$$

$$= \int_0^{\infty} \left[\int_{Tz}^{\infty} f_{Z_0}(z_0|H_1) dz_0 \right] f_{Z_{GO}}(z) dz$$

$$= 1 - \int_0^{\infty} F_{Z_0}(Tz|H_1) f_{Z_{GO}}(z) dz$$

$$= 1 - \int_0^{\infty} \left(1 - \exp\left(-\frac{\beta Tz}{\alpha(1+\text{SCR})}\right)\right) f_{Z_{GO}}(z) dz$$

$$= \int_0^{\infty} \exp\left(-\frac{\beta Tz}{\alpha(1+\text{SCR})}\right) f_{Z_{GO}}(z) dz$$

$$= \int_0^{\infty} \exp\left(-\frac{\beta Tz}{\alpha(1+\text{SCR})}\right) f_{Z_{GO}}(z) dz$$

$$= \frac{2\beta^{N\alpha}}{\Gamma^2(N\alpha)} \int_0^{\infty} z^{N\alpha-1} \gamma(N\alpha, \beta z) \exp\left(-\frac{\beta Tz}{\alpha(1+\text{SCR})} - \beta z\right) dz$$

$$= \frac{2}{\Gamma^2(N\alpha)} \int_0^{\infty} z^{N\alpha-1} \gamma(N\alpha, z) \exp\left(-\left(1 + \frac{T}{\alpha(1+\text{SCR})}\right) z\right) dz$$

This last integral can be solved using equation 3.381.4 of [25], which yields the following closed-form approximation for the P_d of the GO-CAFR detector

$$P_d^{GO} = \frac{2\Gamma(2N\alpha)}{N\alpha\Gamma^2(N\alpha)\left(2 + \frac{T}{\alpha(1+SCR)}\right)^{2N\alpha}} \; {}_2F_1\left(1, 2N\alpha; N\alpha + 1; \frac{1}{2 + \frac{T_{GO}}{\alpha(1+SCR)}}\right) \qquad (2.27)$$

2.6 Conclusion

In this chapter, we first present an overview about CFAR detection of radar signal embedded in homogenous Gamma-distributed clutter. After that, our efforts were focused on studying particularly two well-known Mean-Level CFAR detectors, namely the CA and GO. Indeed, we provide a complete analysis for both detectors. To do so, we present their basic principles and develop their corresponding P_{FA} and P_d expressions. For each detector, the P_{FA} expressions were given in closed-forms, however we propose approximations for the P_D expressions. The performance of both detectors will be analyzed and compared in the last chapter.

Chapiter 3：Results and Discussions

3.1 Introduction

In this last chapter, we will test and examine via simulations the discussed CFAR detectors, namely the CA- and GO-CFAR, which operate over a homogenous GM clutter. First, the different parameters used in our simulations are given. After that, we will validate the proposed expressions of P_{fa} and P_d for both detectors, by comparing them to existing integral expressions and to those obtained by simulations, as well. At the end, the performance of both detectors (i.e, CA- and GO-CFAR) is compared against the well-known optimal fixed threshold detector. The former is included here as a benchmark, since it needs a prior knowledge of clutter parameters.

In the first step, we provide some numerical results to examine and validate the correctness of the proposed expressions (2.16), (2.18), (2.24) and (2.26) for the CA- and the GO-CFAR detectors, respectively. After that, the performance of these detectors is compared to that of the optimal detector.

3.2 Simulation parameters

In order to analyze the performance of the above mentioned CFAR detectors, we propose to carried out several simulations. The influences of changing different parameters on P_{fa} and P_{d}, over the detection performance, is also considered for different simulation scenarios.

The performance of all detectors has been done using both analytical and Monte-Carlo (MC) simulation results. The number of trails for MC simulation is 10^7 and the generated samples were considered independent and identically distributed (IID) according to the Gamma-Distribution. It may be noted that the MC simulation results were included here just for validation purposes.

To this end, a simulated Gamma distributed clutter is generated by considering the shape parameter α equals to 2, 3, and 5. For each value of α, the size of the reference window

for both CFAR detectors is taken to be $2N = 10, 12$, and 16. For each case, the resulted data matrix is of size $2N \times 10^7$, so that it can be assimilated to a CFAR reference window, which is generated 10^7 times. Moreover, the content of the CUT is also generated 10^7 times for both hypothesis H_0 and H_1.

In all considered scenarios, the simulated P_{fa} curves were produced using 10^7 Monte-Carlo simulation trials. For each detector, the decision rules (2.14) and (2.19) was also simulated and the corresponding thresholds were estimated accordingly. To study the P_d performance we consider also a Swerling I or II fluctuating target.

3.3 Validation of our proposed expressions

In this section, we test and validate through several examples the proposed expressions of P_{fa} and P_d. To do this, we provide a comparative analysis between the exact closed-forms P_{fa} and the approximated P_d expressions, and those counterparts calculated using numerical integration and Monte-Carlo simulations.

3.3.1 Validation of P_{fa} expressions

Herin, we validate the expressions of P_{fa} of both CA- and the GO-CFAR detectors. Figures 3.1 – 3.6 illustrate the evolution of the P_{fa} versus the scaling factor T for both detectors, respectively. According to these figures, it is clear that all P_{fa} curves are in excellent agreement for both CA- and GO-CFAR, which confirms our analytical results. In addition, it can be remarked from Figures 3.1 for CA-CFAR and 3.4 for GO-CFAR that the P_{fa} is well maintained whatever the value of β. This conforms the CFAR property of CA- and GO detectors with respect to β. Moreover, according to Figures 3.2, 3.3, 3.5 and 3.6, it is clear that both detectors don't satisfy the CFAR property with respect to α and N.

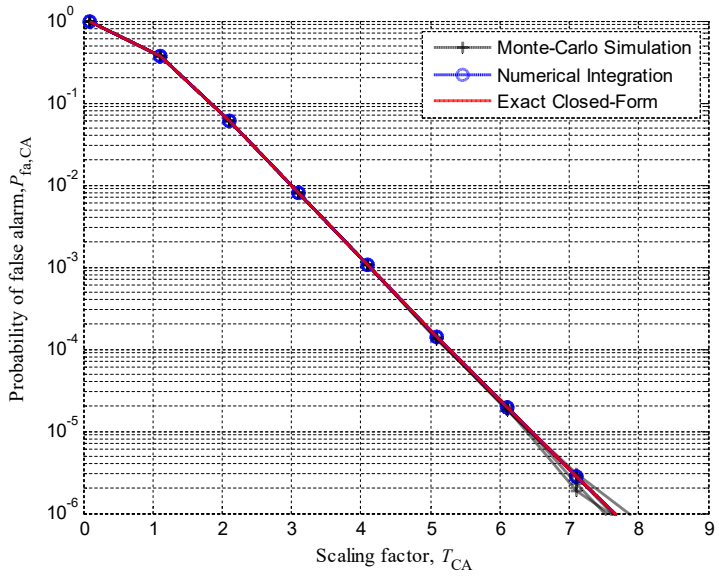

Figure 3.1 - False Alarm Probability of the CA-CFAR detector against the scaling factor T for different values of $\boldsymbol{\beta}$ ($\boldsymbol{\beta} = \mathbf{1}$, $\mathbf{5}$ and $\mathbf{50}$)

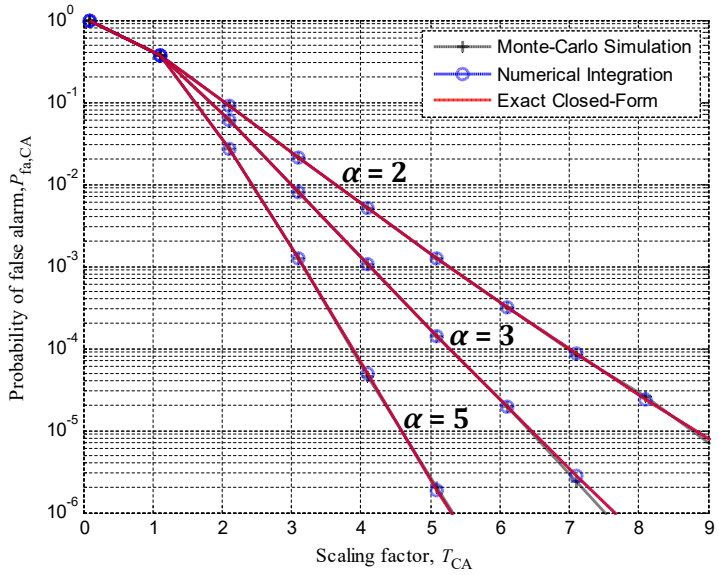

Figure 3.2 - False Alarm Probability of the CA-CFAR detector against the scaling factor T for different values of $\boldsymbol{\alpha}$ ($\boldsymbol{\alpha} = \mathbf{2}$, $\mathbf{3}$ and $\mathbf{5}$)

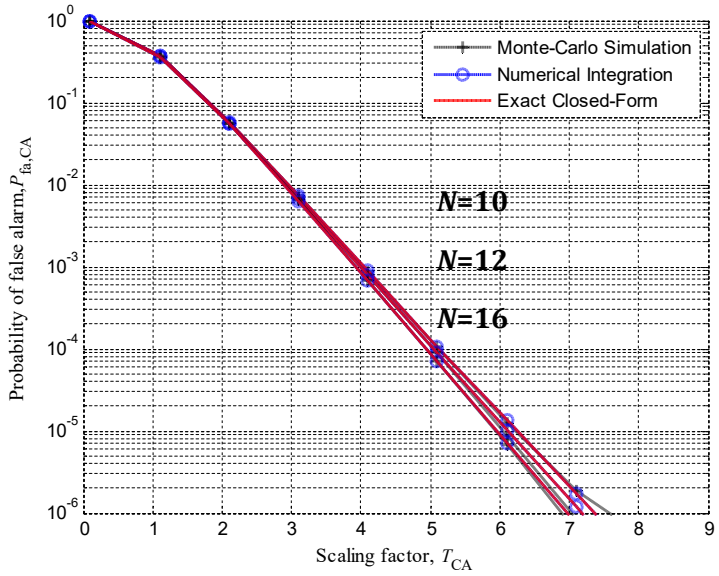

Figure 3.3 - False Alarm Probability of the CA-CFAR detector against the scaling factor T for different values of $\boldsymbol{N}$ ($\boldsymbol{N} = \mathbf{10}$, $\mathbf{12}$ and $\mathbf{16}$)

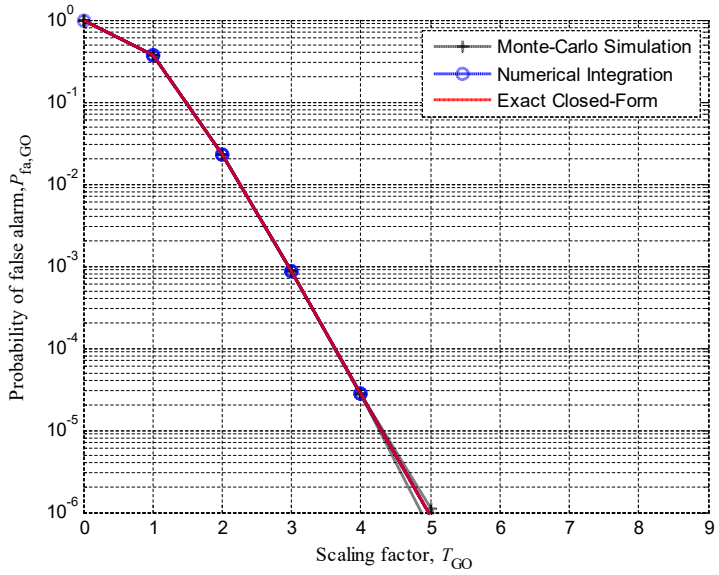

Figure 3.4 - False Alarm Probability of the GO-CFAR detector against the scaling factor T for different values of $\boldsymbol{\beta}$ ($\boldsymbol{\beta} = \mathbf{1}$, $\mathbf{5}$ and $\mathbf{50}$)

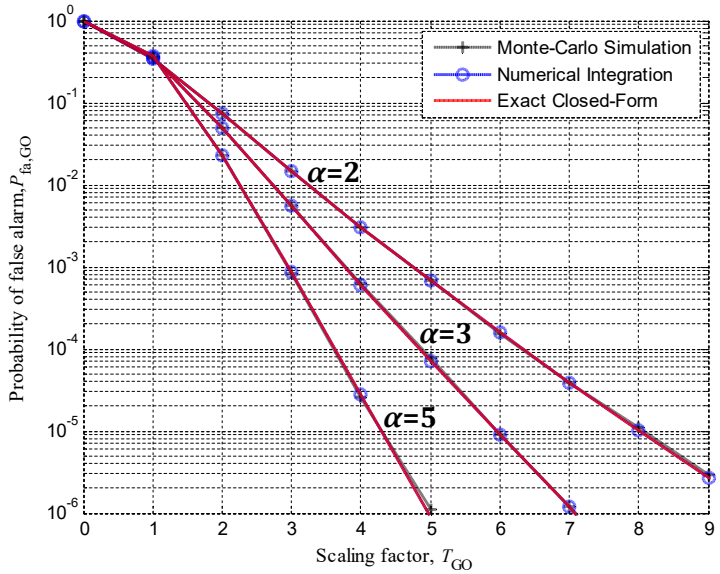

Figure 3.5 - False Alarm Probability of the GO-CFAR detector against the scaling factor T for different values of $\boldsymbol{\alpha}$ ($\boldsymbol{\alpha = 2}$, **3** and **5**)

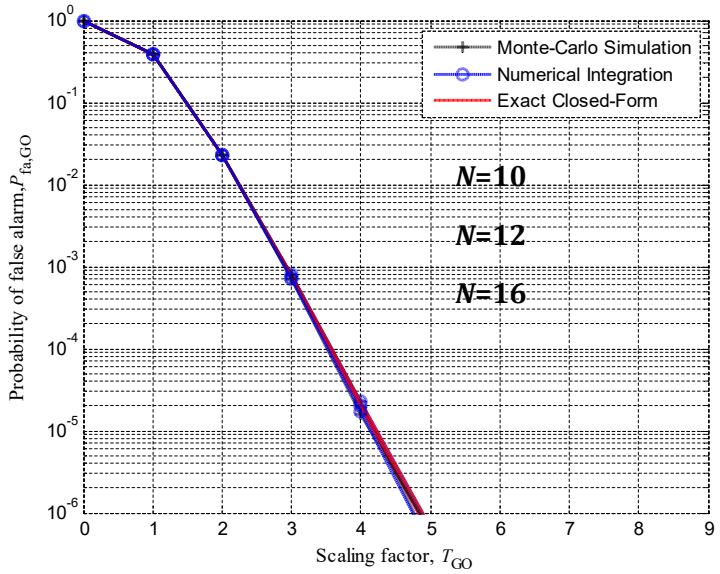

Figure 3.6 - False Alarm Probability of the GO-CFAR detector against the scaling factor T for different values of $\boldsymbol{N}$ ($\boldsymbol{N = 10}$, **12** and **16**)

3.3.2 Validation of P_d expressions

As an initial examination of detection performance, we validate and confirm, in this subsection, our proposed approximation expressions of P_d of both CA and GO-CFAR detectors. In doing that, we compare the approximated P_d with those obtained from Monte-Carlo simulations. The results of both detectors are presented on Figures 3.7 – 3.6. In all cases, performance is measured by plotting the P_d as a function of the Signal-to-Clutter Ratio (SCR), in dB. Monte Carlo sampling with 10^6 runs has been used for each detection probability estimate. The target model used in the CUT is a Swerling I or II as in [16].

All these figures clearly show good agreement between approximate and MC values of P_d curves for both CA- and GO-CFAR detectors. This confirms the effectiveness of the proposed approximation, particularly for relatively high SCR values.

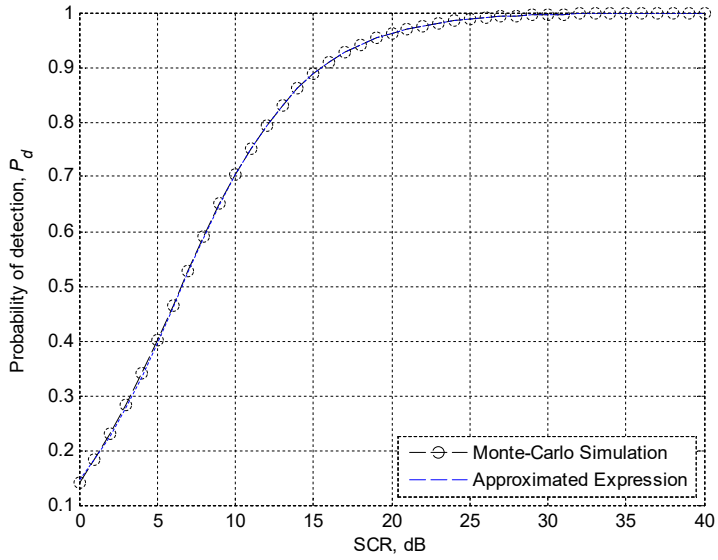

Figure 3.7 - Probability of detection of the CA-CFAR detector against the SCR for $\boldsymbol{\alpha = 3}$, $\boldsymbol{N = 16}$, $\boldsymbol{P_{fa} = 10^{-4}}$ and different values of $\boldsymbol{\beta}$ ($\boldsymbol{\beta = 1}$, **5** and **50**)

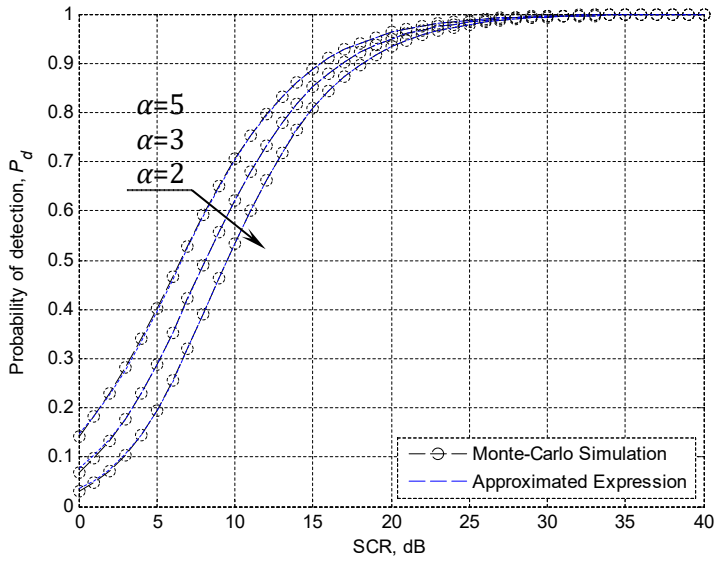

Figure 3.8 - Probability of detection of the CA-CFAR detector against the SCR for $\boldsymbol{N = 16}$, $\boldsymbol{P_{fa} = 10^{-4}}$ and different values of $\boldsymbol{\alpha}$ ($\boldsymbol{\alpha = 2}$, **3** and **5**)

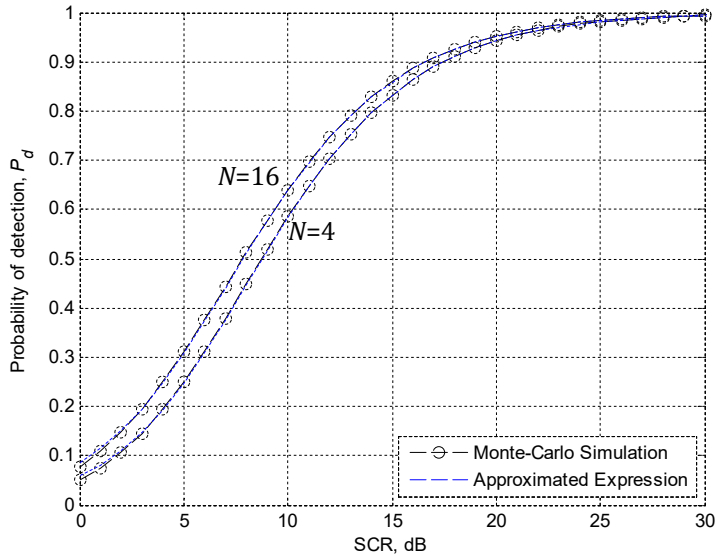

Figure 3.9 - Probability of detection of the CA-CFAR detector against the SCR for $\boldsymbol{\alpha = 3}$, $\boldsymbol{P_{fa} = 10^{-4}}$ and different values of $\boldsymbol{N}$ ($\boldsymbol{N = 4}$ and $\boldsymbol{16}$)

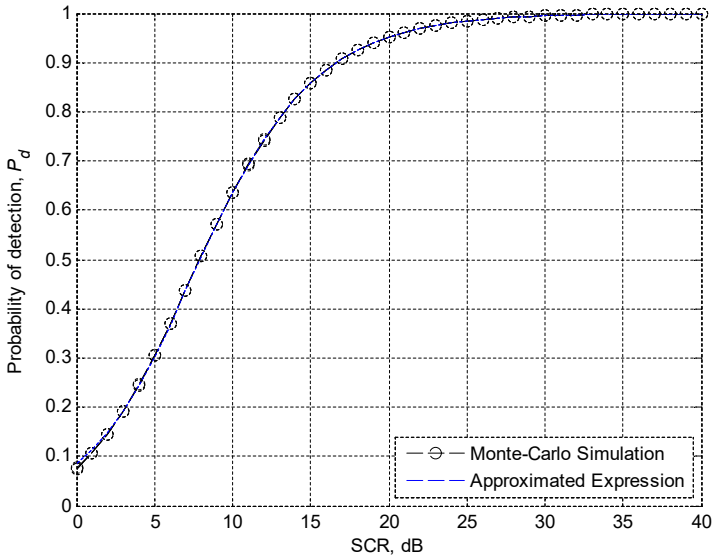

Figure 3.10 - Probability of detection of the GO-CFAR detector against the SCR for $\boldsymbol{\alpha = 3}$, $\boldsymbol{N = 16}$, $\boldsymbol{P_{fa} = 10^{-4}}$ and different values of $\boldsymbol{\beta}$ ($\boldsymbol{\beta = 1}$, $\boldsymbol{5}$ and $\boldsymbol{50}$)

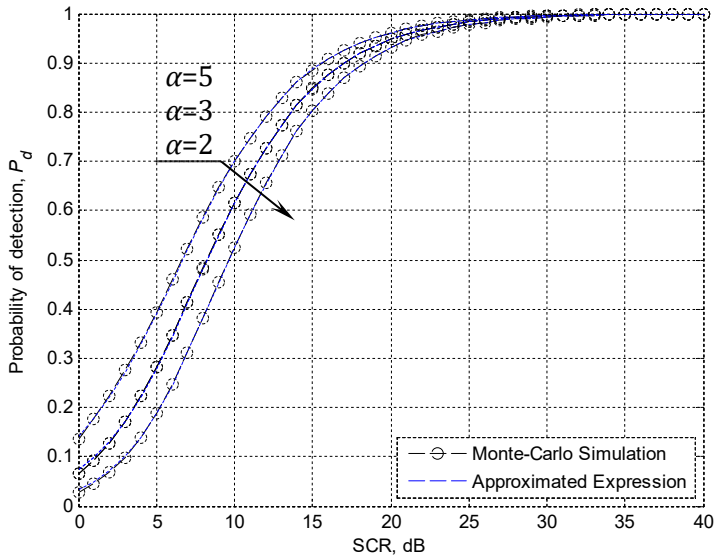

Figure 3.11 - Probability of detection of the GO-CFAR detector against the SCR for $\boldsymbol{N = 16}$, $\boldsymbol{P_{fa} = 10^{-4}}$ and different values of $\boldsymbol{\alpha}$ ($\boldsymbol{\alpha = 2}$, **3** and **5**)

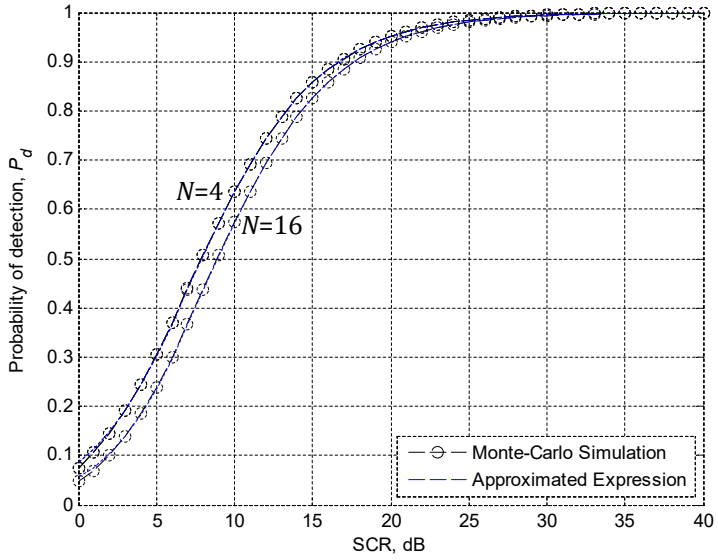

Figure 3.12 - Probability of detection of the GO-CFAR detector against the SCR for $\boldsymbol{\alpha = 3}$, $\boldsymbol{P_{fa} = 10^{-4}}$ and different values of $\boldsymbol{N}$ ($\boldsymbol{N = 4}$ and **16**)

3.4 Comparison of detection performance of CA and GO

Now, we will compare the detection performance of CA and GO-CFAR processors, by assuming the case of homogenous Gamma-Distributed clutter. Several examples of performance will be analyzed by changing some simulation parameters, namely α, N and desired P_{fa}. The optimal detector is also included in these experiments as a benchmark. The obtained results are presented in Figures 3.13, 3.14 and 3.15, respectively.

In Figure 3.13, we study the effect of changing the shape parameter α on the detection performance of the Optimal, CA and GO detectors. In fact, the value of α gives an idea about the spikiness of clutter, where it was observed in practice that the clutter becomes spikier if α decreases and vice-versa (i.e, the clutter becomes less spiky if α increase). Thus, according to this figure, it is evident that the presence of very spiky clutter (i.e, with $\alpha = 2$) introduces a significant detection loss for all detectors. For instance, for $\alpha = 2$ an increase in SCR of about 2dB is required to achieve a $P_d = 0{,}5$ compared with the case where $\alpha = 5$.

On the other hand, we study through Figure 3.14 the effect of increasing the size of the CFAR window, N, on the detection performance of CA and GO processors. We can observe that the detection performance is highly dependent on the value of N. For small N (i.e, $N = 4$) the loss is quite large compared to the optimal detector, but decreases considerably for $N = 16$. For both cases, the performance of the optimal detector remains unaffected. In fact, for $N = 4$, the CFAR loss of CA and GO is about 3dB for a $P_d = 0{,}2$ compared to the optimal scheme, but reduces to less than 0.6dB in the case where $N = 16$.

Figure 3.15 shows the effect of reducing the probability of false alarm P_{fa}. It is interesting to note that the detection performance of all CFAR detectors is good for relatively large false alarm probability ($P_{fa} = \mathbf{10^{-3}}$). However, when P_{fa} is reduced, we can see the substantial performance degradation for all detectors including the optimal.

As a last remark, we can observe also, from Figures 3.13, 3.14 and 3.15, that the detection performance of the CA-CFAR is closer to that of the optimal detector. Moreover, it is clear that the GO-CFAR detector exhibits minor degradation in performance compared to the CA-CFAR.

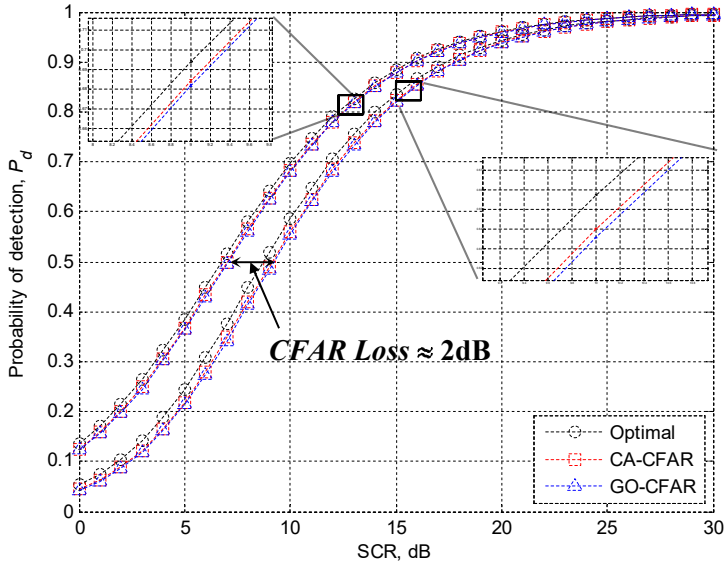

Figure 3.13 - Comparison of detection performance of CA and GO-CFAR detectors for $\boldsymbol{P_{fa} = 10^{-3}}$, $\boldsymbol{N = 16}$ and different values of $\boldsymbol{\alpha}$ ($\boldsymbol{\alpha = 2}$ and $\mathbf{5}$)

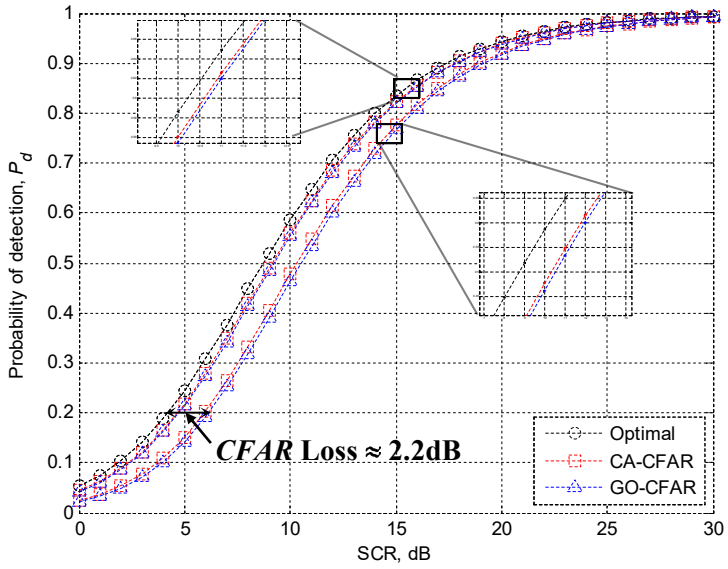

Figure 3.14 - Comparison of detection performance of CA and GO-CFAR detectors for $\boldsymbol{P_{fa} = 10^{-4}}$, $\boldsymbol{\alpha = 2}$ and different values of *N* ($\boldsymbol{N = 4}$ and $\boldsymbol{16}$)

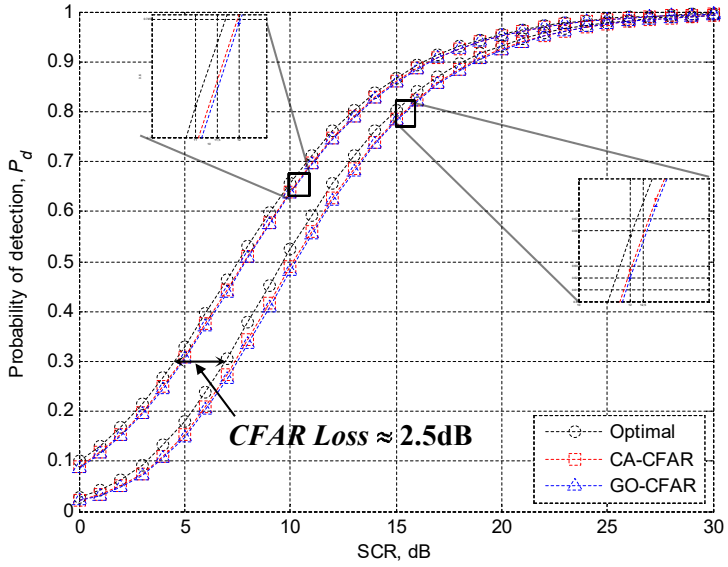

Figure 3.15 - Comparison of detection performance of CA and GO-CFAR detectors for $\boldsymbol{\alpha = 2}$ $\boldsymbol{and}$ $\boldsymbol{N = 16}$ different values of $\boldsymbol{P_{fa}}$ ($\boldsymbol{P_{fa} = 10^{-3}}$ and $\boldsymbol{10^{-5}}$)

3.5 Conclusion

In this chapter, we first tested and validated numerically the closed-form expressions of the false alarm probability and the proposed approximations of detection probability for the CA and GO-CFAR detectors. The obtained results show that all derived expressions agree very well with their counterparts calculated using numerical integration and Monte-Carlo simulations. After that, we studied the detection performance of the Optimal, CA and GO-CFAR algorithms by varying the shape parameter of the Gamma-distribution, the size of the reference window and the desired false alarm probability. The obtained results lead us to conclude that the CA-CFAR detector is effective in homogenous Gamma-Distributed environments.

Conclusion and Perspectives

▪ *Conclusion*

In this master dissertation, we have discussed the problem of CFAR detection of targets embedded in a homogenous Gamma-Distributed clutter. This problem is of great importance in radar systems and remote sensors applications.

Specifically, we focused on studying the performance of two Mean-Level CFAR detectors, namely CA and GO algorithms, by providing a detailed theoretical analysis for each one. The first contribution of this work was presenting two closed-form expressions for the false alarm probability, P_{fa}, for both detectors. It has been shown also that computing the probability of detection, P_d, using exact statistics of the cell under test, results in difficult integrals which are hard to evaluate numerically. Thus, in order to make the analysis easier, we introduced an approximation to the statistics in the cell under test, which leads to obtain two novel approximated expressions for the detection probability for both detectors. It may be noted that our proposed expressions and approximations are easier to compute and to implement in real-time applications.

Our new expressions of P_{fa} and P_d are then tested and validated numerically against their counterparts obtained via numerical integration techniques and Monte-Carlo simulations. Moreover, the performance of CA and GO-CFAR detectors is illustrated and compared to that of the optimal detector. It has been shown that, the CA-CFAR detector offers acceptable performance in a homogenous clutter compared to the GO-CFAR detector, but exhibits some CFAR loss relative to the optimal detector. It has been also demonstrated that the performance of the GO-CFAR is somewhat worse compared to that of the CA-CFAR.

▪ *Perspectives*

The issues addressed in this dissertation are varied, and therefore far from being fully covered in one manuscript. Following the promising results presented here, we can consider different perspectives for future researches, namely:

- A theoretical analysis of CFAR detection performance in the presence of clutter discontinuities and/or interfering targets will be an important topic for further discussion.
- It would also be interesting to analyze and examine the performance of the Smallest Of (SO) CFAR in the presence of a homogenous Gamma-Distributed clutter.
- Similarly, we suggest studying the performance of Multiple pulses detection for the case of a Gamma-distributed clutter.
- It is also worth considering the realistic case where the clutter parameters are completely unknown *a priori*. This will contribute enormously to improve detection performance in non-Gaussian environments.

References

[1] M. Skolnik, Introduction to Radar System, (3rd ed.), New York: McGraw-Hill, 2001.

[2] M. Sahed, *Radar Systems, Course material,* M'Sila: University of M'Sila, 2020.

[3] R. Buderi, The Invention that Changed the World, Touchstone edition, 1998.

[4] E. Jakeman and P. N. Pusey, "A model of non-Rayleigh Sea echo," *IEEE Transactions on Antennas and Propagation,* vol. 24, no. 6, pp. 806-914, 1976.

[5] E. Jakeman and P. Pusey, "Significance of K distributions in scattering experiments," vol. 40, no. 9, p. 546–550, Feb. 1978..

[6] D. K. Ward, "Compound representation of high-resolution sea clutter," *Electronics Letters,* vol. 17, no. 16, pp. 561-563, 1981.

[7] M. Sahed, E. Kenane, A. Khalfa and F. Djahli, "Exact Closed-Form Pfa Expressions for CA- and GO-CFAR Detectors in Gamma-Distributed Radar Clutter," *IEEE Trans. Aerosp. Electron. Syst,* vol. Doi: 10.1109/TAES.2022.3232101., 2023.

[8] F. D. A. García, A. C. F. Rodriguez, G. Fraidenraich and J. C. S. S. Filho, "CA-CFAR Detection Performance in Homogeneous Weibull Clutter," *Remote. Sens. Lett,* vol. 16, no. 4, p. 887–891, Jun. 2019.

[9] C. Schleher, "Radar detection in Weibull clutter," *IEEE Transactions on Aerospace and Electronic Systems,* vol. 12, no. 6, pp. 736-743, 1976.

[10] M. Guida, M. Longo and M. Lops, "Biparametric CFAR procedures for lognormal clutter," *Aerosp. Electron. Syst,* vol. 29, no. 3, p. 798–809, Jul. 1993.

[11] W. Zhou, J. Xie, G. Li and Y. Du, "Robust CFAR detector with weighted amplitude iteration in nonhomogeneous sea clutter," *Aerosp. Electron. Syst,* vol. 53, no. 3, p. 1520–1535, Jun. 2017.

[12] S. Kay, Fundamental Of Statistical Signal Processing: Detection Theory, Englwood Cliffs: Prentice Hall, 1998.

[13] M. Sahed, "Détection Automatique CFAR en environnement Non Gaussien,"," Thèse de Doctorat ès science, Université de M'sila, 2015.

[14] P. A, "On adaptive censored CFAR detection," Thèse de Doctorat, New Jersey Institute of Technology, 1993.

[15] P. Gandhi and S. A. Kassam, "Optimality of the cell averaging CFAR detector," *IEEE*

Transactions on Information Theory, vol. 40, no. 4, pp. 1226-1228, 1994.

[16] P. P. Gandhi and S. A. Kassam, "Analysis of CFAR processors in nonhomogeneous background," *IEEE Transactions on Aerospace and Electronic Systems,* vol. 24, no. 4, pp. 427-445, 1988.

[17] S. Watts, "Cell-averaging CFAR gain in spatially correlated K-distributed clutter," *Radar, Sonar and Navigation,* vol. 143, no. 5, p. 321–327, Oct. 1996..

[18] G. Minkler and J. Minkler, CFAR – the principles of automatic radar detection in clutter, Baltimore: Magellan, 1990.

[19] M. Sahed, "Détection CFAR dans un clutter de mer de distribution K avec des paramètres inconnus en présence du bruit thermique," Mémoire de Magistère, Université de M'sila, Algérie., 2010.

[20] S. George, The detection of nonfluctuating targets in log-normal clutter, Washington, DC, USA,: Naval Research Laboratory., Oct. 1968..

[21] K. Krishnamoorthy, Handbook of Statistical Distributions with Applications,", USA: Chapman & Hall/CRC, 2006.

[22] F. Gini, F. Lombardini and L. Verrazzani, "Decentralized CFAR detection with binary integration in Weibull clutter," *IEEE Trans. Aerosp. Electron. Syst.,* vol. 33, no. 2, pp. 396-407, Apr. 1997.

[23] R. Ravid and N. Levanon, "Maximum-likelihood CFAR for Weibull background," *IEE Proceedings, Radar, Sonar and Navig.,* vol. 139, no. 3, pp. 256-264, Jun. 1992..

[24] M. Abramowitz and I. A. Stegun, Handbook of Mathematical Functions, New York: Dover Publications, Inc., 1970.

[25] I. S. Gradshteyn and I. M. Ryzhik, Table of Integrals, Series, and Products, San Diego: Academic Press, 2015.

[26] H. M. F. a. R. S. A. Johnson, "Adaptive detection model with threshold control as function of spatially sampled clutter-level estimates," *RCA Rev,* vol. 29, p. 414–464, 1968.

[27] S. B. Opps, N. Saad and H. M. Srivastava, "Some reduction and transformation formulas for the Appell hypergeometric function F2," *J. Math. Anal. Appl,* Vols. 302,, no. 1, pp. 180-195, Feb. 2005..

Abstract **—** In this study, we addressed the problem of adaptive detection of radar targets in a homogenous Gamma-distributed clutter. This type of detection is achieved by maintaining a Constant False Alarm Rate (CFAR) during the detection process. We assume that the radar uses a square-law device before the CFAR processor window. First of all, we present the fundamentals of radar detection of targets embedded in noise and giving the basics of CFAR detection. After that, we discuss in more details some Mean-Level CFAR detectors operating over a Gamma-distributed clutter, namely the CA- and GO-CFAR detectors. To do so, we carried out a complete theoretical analysis of both detectors. Indeed, closed-form expressions for the probability of false alarm (P_{fa}) have been presented for each detector. The calculation of the probability of detection (P_d), using the exact statistics of the cell under test (CUT), results in complicated integrals, which are hard to evaluate numerically. Thus, we propose approximate expressions for the probability of detection (P_d) for both detectors. These expressions and approximations are easier to compute and straightforwardly implementable in real-time applications. The obtained theoretical results are then tested and validated numerically by comparing them to their counterparts computed using numerical integrals and Monte-Carlo simulations, considering various scenarios. Moreover, a performance comparison of the studied detectors with the optimal detector has been made assuming a homogenous environment. The obtained results confirmed the efficacy of the CA-CFAR detector in the case of homogeneous environments.

Keywords: Radar, Adaptative CFAR detection, non-Gaussian Clutter, Gamma-Distribution, CA-CFAR, GO-CFAR.

ملخص — ناقشنا من خلال هذه الدراسة مسألة الكشف عن الأهداف المهمة المتواجدة في وسط (محيط) متجانس، بحيث تكون الاشارات العشوائية الناتجة عن هذا الوسط موزعةً توزيعًا احصائيًا غير طبيعيٍ حسب نموذج غاما (Gamma model). حيث قمنا باستعمال تقنية الكشف التكيفي بنسبة إنذار خاطئ ثابتة (CFAR Detection)، باعتبارها وسيلة ناجعة في مثل هذه الأوساط سريعة التغير. في البداية، أجرينا دراسةً نظرية وتحليليةً كاملةً للكاشفات التي تعتمد على حساب المتوسط الحسابي المعروفة بـ Mean-Level CFAR Detectors، مثل الكاشف CA-CFAR و الكاشف GO-CFAR. الدراسة التحليلية لهذين الكاشفين سمحت لنا كذلك بحساب العبارات التحليلية لاحتمال الإنذار الخاطئ (Probability of False Alarm) وكذا حساب عبارات مقربة لاحتمال الكشف (Probability of detection). تتميز العبارات والتقريبات المقترحة بسهولة الحساب وقابلية البرمجة والتنفيذ بشكل سهل وبسيط في التطبيقات الحقيقية لأجهزة الرادار. بعد ذلك قمنا بفحص النتائج النظرية المحصل عليها وكذا التحقق من صحتها باستعمال المحاكاة الرقمية، من خلال مقارنتها مع نظيراتها المحسوبة باستخدام التكاملات العددية وتلك المحصل عليها عن طريق محاكاة مونت كارلو (Monte-Carlo Simulation). من خلال عمليات المحاكاة الرقمية أيضا، قمنا بمقارنة واختبار أداء الكاشفين CA و GO الذين تمت دراستها ومناقشتها في هذا العمل مع الكاشف المثالي. حيث أكدت النتائج المتحصل عليها على نجاعة الكاشف CA-CFAR في حالة وجود أوساط متجانسة.

الكلمات المفتاحية: الرادار، الكشف المكيف بنسبة إنذار خاطئ ثابتة، التشويش الغير غاوسي(الغير طبيعي)، توزيع غاما، CA-، GO-CFAR.